Quantum theory of high-energy electron transport in the surface region

K. L. Aminov* and J. Boiden Pedersen
Fysisk Institut, Syddansk Universitet, DK-5230 Odense M, Denmark
(Received 3 November 2000; published 13 March 2001)

A quantum Boltzmann's equation is derived to describe the transport of high-energy electrons in spatially inhomogeneous media. In the lowest approximation this equation reduces to a local Boltzmann's equation where the scattering function is expressed in terms of a generalized dielectric function of the media. The inelastic scattering of high-energy electrons near the surface of the solid is investigated by use of the local Boltzmann's equation. For a solid with an abrupt surface and a nondispersive dielectric function the inelastic-scattering function shows an oscillatory behavior in the surface region that can be explained as a resonant interaction of the electron with its image. Numerical calculations of the scattering function for several previously introduced models for a solid with a dispersive dielectric function are also presented. The calculated results indicate that the oscillatory behavior near the surface is a general phenomenon. Moreover, it is found that the inelastic-scattering function depends significantly on the surface model. A proper choice of model is therefore a prerequisite for a correct interpretation of experimental energy-loss spectra.

DOI: 10.1103/PhysRevB.63.125412 PACS number(s): 73.40.−c, 72.10.Bg, 73.50.Bk

I. INTRODUCTION

In recent years electron spectroscopy has become an important tool for investigating properties of solids, particularly in the surface region.[1–5] Because of the limited penetration depth of the electron, the spectral information refers to a surface layer usually not exceeding 100 Å in depth. It is well-established experimentally that surface excitations contribute with significant features to the electron spectrum for energies below 1 keV. These effects are more prominent for low electron energies since the mean free path, and thus the penetration depth, of the electron decreases with decreasing electron energy. A quantitative analysis of low-energy electron spectra therefore necessitates a proper treatment of the interaction of electrons with surface excitations.

Many authors[6–11] have used a Boltzmann-type transport equation as a basis for quantitative interpretations of electron spectra obtained by various spectroscopical techniques such as x-ray photoelectron spectroscopy (XPS), Auger electron spectroscopy (AES), and reflected-electron-energy-loss spectroscopy (REELS). In these approaches the elastic-scattering processes are treated by means of electron-atom scattering cross sections and it is assumed that the angular deflections due to inelastic-scattering processes can be neglected for high electron energies. The inelastic scattering is therefore described by a differential inverse inelastic mean-free-path (DIMFP) which for the bulk of the solid can be expressed in terms of the loss function $-\mathrm{Im}[\varepsilon^{-1}(\mathbf{q},\omega)]$, where $\varepsilon(\mathbf{q},\omega)$ is the dielectric function of the solid.[12,13] Surface scattering is neglected and it is assumed that the inelastic-scattering properties of the solid are homogeneous within the bulk volume and up to the surface. For energy losses much smaller than the electron energy the solution of the transport equation can be then written[6] as a convolution of the path distribution function of the electrons in the solid with the Landau energy-loss function[14] expressed via the bulk differential inverse inelastic mean free path (DIMFP).

Earlier solutions to the problem of electron scattering by the surface of a solid[13,15–18] show that the effect of the surface on the electron energy loss can be described by the surface loss function, which in the case of nondispersive solid, has the form $\mathrm{Im}\{-1/[\varepsilon(\omega)+1]\}$.[13,15] In the single-plasmon model of a solid with bulk plasmon frequency ω_0 this form reproduces a peak with a frequency $\omega_0/\sqrt{2}$ corresponding to surface-plasmon excitations. In a solid with spatial dispersion of the dielectric function the surface loss function becomes more complicated and, in general, the scattering properties of the surface has to be expressed by a generalized dielectric function $\varepsilon(\mathbf{q},\mathbf{k};\omega)$ of the spatially inhomogeneous solid.[16–18]

In order to include the interaction with surface excitations into the transport equation the spatial dependence of the inelastic-scattering probabilities near the surface must be considered. Previously, there have been several attempts to obtain the spatial dependence of the scattering function from calculations of the stopping power for electrons moving along classical trajectories.[19–22] However, the relation between the scattering function obtained by these approaches and the transport equation has not been clarified.

The aim of the present paper is to derive, from first principles, a transport equation for high-energy electrons in solids where the effects of spatial inhomogeneities of the solid (such as the surface) on the inelastic-scattering properties are taken into account self-consistently.

In Sec. II we derive a quantum Boltzmann's equation (QBE) for transport of high-energy electrons interacting with the solid. This general equation is then approximated by a transport equation with local inelastic-scattering probabilities. The spatially varying scattering functions and the DIMFP are expressed in terms of a generalized dielectric function of the solid.

In Sec. III we apply the expressions derived in Sec. II to transport of high-energy electrons in the surface region. By using a simple model for a nondispersive solid we obtain an explicit analytical expression for the spatial dependence of the scattering function, which displays an oscillating behavior near the surface. This phenomenon can be explained as the effect of the resonant interaction of the electron with its

image. Calculations of the DIMFP for transport along the surface normal are also performed for two previous surface models, that use dispersive solids[23,19,22] It is demonstrated that the scattering properties of the surface depend significantly on the choice of the surface model.

In Sec. IV a quantitative analysis of surface effects in electron energy-loss spectra is discussed in terms of the differential surface excitation parameter. An algorithm for retrieving this parameter from REELS spectra is proposed.

Finally, in Sec. V we compare the results of our theory with those derived from the quasiclassical approach based on stopping-power calculations.

II. TRANSPORT EQUATION

A quantum theory describing the transport of high-energy electrons interacting with a solid has recently been developed by Dudarev *et al.*[24] In this section we reformulate their basic transport equation in the form of a QBE. The quasiclassical limit of this equation is then used to derive a spatially inhomogeneous inelastic-scattering function for noncrystalline solids.

The Hamiltonian of the high-energy electrons interacting with the solid can be written as

$$H=\int d^3r\,\psi^\dagger(\mathbf{r})\left[-\frac{\hbar^2}{2m}\nabla_{\mathbf{r}}^2+V(\mathbf{r})\right]\psi(\mathbf{r})+H_s, \quad (2.1)$$

where $\psi^\dagger$ and ψ are creation and annihilation operators, respectively, of the high-energy electrons, $V(\mathbf{r})$ is the interaction potential of the solid acting on the electron at the point $\mathbf{r}$, and H_s is the Hamiltonian of the solid.

For a solid in thermodynamical equilibrium, the potential can be separated into a static part and a dynamic parts as

$$V(\mathbf{r})=\langle V(\mathbf{r})\rangle+\delta V(\mathbf{r}). \quad (2.2)$$

Here $\langle\ldots\rangle$ denotes an average with the equilibrium density operator, which in Dirac notation has the form

$$\rho_0=\frac{1}{Z}\sum_s \exp(-\epsilon_s/k_BT)|s,0\rangle\langle s,0|, \quad (2.3)$$

where the combined state $|s,0\rangle$ indicates that the solid is in an eigenstate $|s\rangle$ with energy ϵ_s and the electron is in the vacuum state, $Z=\Sigma_s\exp(-\epsilon_s/k_BT)$ is the partition function, T is the temperature, and k_B is Boltzmann's constant.

The static part $\langle V(\mathbf{r})\rangle$ is responsible for the elastic scattering of the electrons by the atoms of the solid situated in their average or equilibrium positions. The fluctuating part of the potential $\delta V(\mathbf{r})$ is responsible for the inelastic scattering of the electrons, which is caused by the interaction of the electrons with the excitations of the solid. For noncrystalline solids the elastic- and inelastic-scattering parts can usually be treated separately. [6–11] Therefore, for the sake of simplicity, we will neglect the static part of the potential and assume that the elastic scattering can be included in the quasiclassical Boltzmann's equation at a later stage. The form of the elastic-scattering term in the transport equation is well-known for noncrystalline solids, see e.g., Ref. 11.

The basic entity in the theory, which is directly related to experimentally measured quantities, is the bilinear combination of the electron's wave functions, which can be written as a nonequilibrium correlation function

$$\rho(\mathbf{r},t;\mathbf{r}',t')=\langle\psi^\dagger(\mathbf{r}',t')\psi(\mathbf{r},t)\rangle_{\rm ne}, \quad (2.4)$$

where $\langle\ldots\rangle_{\rm ne}$ denotes an average with the nonequilibrium density operator, and the time dependence of the operators $\psi^\dagger$ and ψ is given by $\psi(t)=\exp(iHt/\hbar)\psi\exp(-iHt/\hbar)$. The creation of the high-energy electrons in the solid can be described by a source function $I(\mathbf{r}_0,t_0;\mathbf{r}_0',t_0')$ such that the evolution of the created electrons can be written as

$$\rho(\mathbf{r},t;\mathbf{r}',t')=\int_{-\infty}^{\infty}dt_0\int_{-\infty}^{\infty}dt_0'\int d^3r_0\int d^3r_0' \times K(\mathbf{r},t;\mathbf{r}',t'|\mathbf{r}_0,t_0;\mathbf{r}_0',t_0')I(\mathbf{r}_0,t_0;\mathbf{r}_0',t_0'), \quad (2.5)$$

where

$$K(\mathbf{r},t;\mathbf{r}',t'|\mathbf{r}_0,t_0;\mathbf{r}_0',t_0')=\theta(t-t_0)\,\theta(t'-t_0')\langle\psi(\mathbf{r}_0',t_0') \times\psi^\dagger(\mathbf{r}',t')\psi(\mathbf{r},t)\psi^\dagger(\mathbf{r}_0,t_0)\rangle \quad (2.6)$$

is the two-particle Green's function for the electron.

Another function, which must be calculated in order to solve the transport problem, is the single electron Green's function, which is defined as

$$G(\mathbf{r},\mathbf{r}'|t-t')=-i\,\theta(t-t')\langle\psi(\mathbf{r},t)\psi^\dagger(\mathbf{r}',t')\rangle. \quad (2.7)$$

Note that only the time difference is used as argument in the Green's function (2.7) since we have chosen the vacuum state of the high-energy electron as the thermodynamic equilibrium.

It is possible to derive equations for the two Green's functions G and K by applying diagrammatic methods to a calculation of the nonequilibrium contour-ordered correlation functions.[25] The equations obtained in Ref. 24 can then be modified as follows. The single-particle Green's function (2.7) satisfies a Dyson equation which, can be written as

$$\left[i\frac{\partial}{\partial t}+\frac{\hbar}{2m}\nabla_{\mathbf{r}}^2\right]G(\mathbf{r},\mathbf{r}'|t)-\int d^3x\int dt'\,G(\mathbf{r},\mathbf{x}|t') \times S(\mathbf{r},\mathbf{x}|t')G(\mathbf{x},\mathbf{r}'|t-t') =\delta(\mathbf{r}-\mathbf{r}')\,\delta(t), \quad (2.8)$$

where

$$S(\mathbf{r},\mathbf{r}'|t')=\frac{1}{\hbar^2}\langle\exp(iH_st/\hbar)\,\delta V(\mathbf{r})\exp(-iH_st/\hbar)\,\delta V(\mathbf{r}')\rangle \quad (2.9)$$

is the equilibrium correlation function of the fluctuations of the solid potential. Note that in Eq. (2.8) the self-consistent Born approximation is used for the self-energy and both Green's functions in the integrand appear ''dressed,'' which

makes the equation different from the corresponding Eq. (10) in Ref. 24. The use of ''dressed'' Green's functions makes the transition to the QBE more consistent (see below).

An equation for the two-particle Green's function (2.6) may be found in Ref. 24, Eq. (B10), which may be written as

$$\begin{aligned} K(\mathbf{r},t;\mathbf{r}',t'|\mathbf{r}_0,t_0;\mathbf{r}_0',t_0') &= G(\mathbf{r},\mathbf{r}_0|t-t_0)G^*(\mathbf{r}',\mathbf{r}_0'|t'-t_0') \\ &+ \int d\tau \int d\tau' \int d^3x \int d^3x' G(\mathbf{r},\mathbf{x}|t-\tau) \\ &\times G^*(\mathbf{r}',\mathbf{x}'|t'-\tau')S(\mathbf{x}',\mathbf{x}|\tau'-\tau) \\ &\times K(\mathbf{x},\tau;\mathbf{x}',\tau'|\mathbf{r}_0,t_0;\mathbf{r}_0',t_0'). \end{aligned} \tag{2.10}$$

Our aim is to obtain a closed form of the QBE for the Wigner distribution function, which is related to the density correlation function (2.4) as

$$\rho(\mathbf{k},\omega;\mathbf{R},T) = \int d^3r \int dt e^{i(\omega t-\mathbf{kr})}\rho \times\left(\mathbf{R}+\frac{\mathbf{r}}{2},T+\frac{t}{2};\mathbf{R}-\frac{\mathbf{r}}{2},T-\frac{t}{2}\right). \tag{2.11}$$

First, we use Eq. (2.8) and its complex conjugate to eliminate G or G^* from the right-hand side of Eq. (2.10). By taking the difference between the resulting integro-differential equations and using Eq. (2.5) we obtain an equation for the density distribution function (2.4) in the form

$$\begin{aligned} &\left[i\left(\frac{\partial}{\partial t}+\frac{\partial}{\partial t'}\right)+\frac{\hbar}{2m}(\nabla_{\mathbf{r}}^2-\nabla_{\mathbf{r}'}^2)\right]\rho(\mathbf{r},t;\mathbf{r}',t') - \int d^3x \int d\tau[G(\mathbf{r},\mathbf{x}|t-\tau)S(\mathbf{r},\mathbf{x}|t-\tau)-G(\mathbf{r},\mathbf{x}|t-\tau)S(\mathbf{r}',\mathbf{x}|t'-\tau)] \\ &\times\rho(\mathbf{x},\tau;\mathbf{r}',t') - \int d^3x \int d\tau[G^*(\mathbf{r}',\mathbf{x}|t'-\tau)S(\mathbf{x},\mathbf{r}|\tau-t)-G^*(\mathbf{r}',\mathbf{x}|t'-\tau)S(\mathbf{x},\mathbf{r}'|\tau-t')]\rho(\mathbf{r},t;\mathbf{x},\tau) \\ &= \int d^3x \int d\tau[G^*(\mathbf{r}',\mathbf{x}|t'-\tau)I(\mathbf{r},t;\mathbf{x},\tau)-G(\mathbf{r},\mathbf{x}|t-\tau)I(\mathbf{x},\tau;\mathbf{r}',t')]. \end{aligned} \tag{2.12}$$

The following steps towards a quasiclassical Boltzmann's equation are identical to those used in nonequilibrium Green's functions theory.[25,26] New independent variables $T=(t_1+t_2)/2$, $\mathbf{R}=(\mathbf{r}_1+\mathbf{r}_2)/2$, $t=t_1-t_2$, and $\mathbf{r}=\mathbf{r}_1-\mathbf{r}_2$ are introduced into Eq. (2.12) and Fourier transformations over the $\mathbf{r}$ and t variables, as in Eq. (2.11), are performed. The integrals in Eq. (2.12) are transformed according to the identity

$$\begin{aligned} &\int d^3x \int d\tau A(\mathbf{r}_1,t_1;\mathbf{x},\tau)B(\mathbf{x},\tau;\mathbf{r}_2,t_2) \\ &\rightarrow \exp[i(\partial_\omega^A\partial_T^B-\partial_T^A\partial_\omega^B-\nabla_{\mathbf{k}}^A\nabla_{\mathbf{R}}^B+\nabla_{\mathbf{R}}^A\nabla_{\mathbf{k}}^B)/2]A(\mathbf{k},\omega;\mathbf{R},T) \\ &\times B(\mathbf{k},\omega;\mathbf{R},T). \end{aligned} \tag{2.13}$$

If we assume that the functions vary slowly with $\mathbf{R}$ and T then we may neglect all but the lowest term in the expansion of Eq. (2.13) and obtain

$$\begin{aligned} &\left[\frac{\partial}{\partial T}+\mathbf{v}_k\nabla_{\mathbf{R}}+\int\frac{d\omega'}{2\pi}\int\frac{d^3k'}{(2\pi)^3}A(\mathbf{k}',\omega';\mathbf{R}) \times S(\mathbf{k}-\mathbf{k}',\omega-\omega';\mathbf{R})\right]\rho(\mathbf{k},\omega;\mathbf{R},T) \\ &-\int\frac{d\omega'}{2\pi}\int\frac{d^3k'}{(2\pi)^3}A(\mathbf{k},\omega;\mathbf{R}) \times S(\mathbf{k}'-\mathbf{k},\omega'-\omega;\mathbf{R})\rho(\mathbf{k}',\omega';\mathbf{R},T) \\ &= A(\mathbf{k},\omega;\mathbf{R})I(\mathbf{k},\omega;\mathbf{R},T), \end{aligned} \tag{2.14}$$

where $\mathbf{v}_{\mathbf{k}}=\hbar\mathbf{k}/2m$ is the velocity of the electron, and

$$A(\mathbf{k},\omega;\mathbf{R}) \equiv i[G(\mathbf{k},\omega;\mathbf{R})-G^*(\mathbf{k},\omega;\mathbf{R})] \tag{2.15}$$

is the spectral intensity function of the electron. We replace this function by its free-electron value $A_0(\mathbf{k},\omega;\mathbf{R})=2\pi\delta(\omega-\epsilon_k)$ with $\epsilon_k\equiv\hbar k^2/2m$. In the limit where the quasiclassical approximation is valid the function ρ can be approximated by

$$\rho(\mathbf{k}',\omega';\mathbf{R},T)\simeq 2\pi\delta(\omega-\epsilon_k)\rho(\mathbf{k},\mathbf{R};T), \tag{2.16}$$

where $\rho(\mathbf{k},\mathbf{R};T)$ is the quasiclassical electron-density distribution function. By integrating Eq. (2.14) over ω we finally obtain the Boltzmann's equation in the form

$$\begin{aligned} &\left[\frac{\partial}{\partial t}+\mathbf{v}_{\mathbf{k}}\nabla_{\mathbf{r}}+\tau_{\mathbf{k}}^{-1}(\mathbf{r})\right]\rho(\mathbf{k},\mathbf{r};t)-\int\frac{d^3k'}{(2\pi)^3}W_{\mathbf{kk}'}(\mathbf{r})\rho(\mathbf{k}',\mathbf{r};t) \\ &= I(\mathbf{k},\mathbf{r};t), \end{aligned} \tag{2.17}$$

where

$$\tau_{\mathbf{k}}^{-1}(\mathbf{r})=\int\frac{d^3k'}{(2\pi)^3}W_{\mathbf{k}'\mathbf{k}}(\mathbf{r}) \tag{2.18}$$

is the inverse mean time between inelastic-scattering events, and the inelastic-scattering function

$$W_{\mathbf{k}\mathbf{k}'}(\mathbf{r}) = \int_{-\infty}^{\infty} dt \int d^3x \exp[i(\epsilon_{k'} - \epsilon_k)t - i(\mathbf{k}' - \mathbf{k})\mathbf{x}] \times S\left(\mathbf{r} + \frac{\mathbf{x}}{2}, \mathbf{r} - \frac{\mathbf{x}}{2}\middle| t\right), \tag{2.19}$$

where S is defined in Eq. (2.9). By using the relation[27] between the correlation function (2.9) of the solid potential fluctuations and the inverse generalized dielectric function we can express the inelastic-scattering function (2.19) as

$$W_{\mathbf{k}'\mathbf{k}}(\mathbf{r}) = -\frac{8\pi e^2}{\hbar}\theta(\epsilon_k - \epsilon_{k'})\mathrm{Im}\left[\int \frac{d^3q}{(2\pi)^3} e^{i\mathbf{q}\mathbf{r}} \frac{\varepsilon^{-1}\left(\mathbf{k} - \mathbf{k}' + \frac{\mathbf{q}}{2}, \mathbf{k} - \mathbf{k}' - \frac{\mathbf{q}}{2}\middle| \epsilon_k - \epsilon_{k'}\right)}{\left(\mathbf{k} - \mathbf{k}' - \frac{\mathbf{q}}{2}\right)^2}\right], \tag{2.20}$$

where e is the charge of the electron and the inverse generalized dielectric function is defined by

$$\phi(\mathbf{q}, \omega) = \int \frac{d^3q'}{(2\pi)^3} \varepsilon^{-1}(\mathbf{q}, \mathbf{q}'|\omega)\phi_{\mathrm{ext}}(\mathbf{q}', \omega), \tag{2.21}$$

where ϕ_{ext} and ϕ are the scalar potentials of the external and the induced electric fields.

For large electron energies, the angular deflections of the electron's trajectory due to inelastic-scattering processes are small and are usually neglected. The effects of the inelastic scattering for that case are described by an energy-loss function also known as the DIMFP. We denote this probability density $K(E, \mathbf{r}, \phi; \hbar\omega)$ for an electron at position $\mathbf{r}$, having an energy E, and moving in the direction ϕ, to loose energy $\hbar\omega$ in the next inelastic-scattering event. In analogy with the inverse mean-free-time defined in Eq. (2.18) we obtain

$$K(\hbar\epsilon_k, \mathbf{r}, \phi_{\mathbf{k}}; \hbar\omega) = \frac{1}{v_k}\int \frac{d^3k'}{(2\pi)^3}\delta(\hbar\epsilon_k - \hbar\epsilon_{k'} - \hbar\omega) \times W_{\mathbf{k}'\mathbf{k}}(\mathbf{r}), \tag{2.22}$$

where $\phi_{\mathbf{k}}$ defines the direction of the vector $\mathbf{k}$, i.e., the direction of the trajectory before the collision. Substitution of Eq. (2.20) into Eq. (2.22) leads to

$$K(\hbar\epsilon_k, \mathbf{r}, \phi_{\mathbf{k}}; \hbar\omega) = -\frac{8\pi e^2}{\hbar^2 v_k}\theta(\omega)\int \frac{d^3q}{(2\pi)^3}\int \frac{d^3q'}{(2\pi)^3} \times \frac{\delta(\epsilon_k - \epsilon_{\mathbf{k}-(\mathbf{q}+\mathbf{q}')/2} - \omega)}{q'^2}\mathrm{Im}\{\varepsilon^{-1}(\mathbf{q}, \mathbf{q}'|\omega) \times \exp[i(\mathbf{q} - \mathbf{q}')\mathbf{r}]\}. \tag{2.23}$$

Equations (2.20) and (2.23) represent our results for the inelastic-scattering function that enters the Boltzmann's limit of the transport equation for a spatially inhomogeneous solid. For the homogeneous case

$$\varepsilon^{-1}(\mathbf{q}, \mathbf{q}'|\omega) = (2\pi)^3\delta(\mathbf{q} - \mathbf{q}')\varepsilon^{-1}(\mathbf{q}, \omega) \tag{2.24}$$

and Eqs. (2.20) and (2.23) simplify to the well-known previous expressions.[13,28]

III. INELASTIC SCATTERING IN THE SURFACE REGION

In this section we treat the transport of high-energy electrons in the near-surface region of noncrystalline solids using the inelastic-scattering function for the spatially inhomogeneous solid derived in the previous section. We choose the surface to be the plane $z = 0$ with the bulk of the solid extending in the direction $z < 0$. Also, for the simplicity, we assume that the solid is invariant with respect to rotations around the z axis. With this geometry, the inverse generalized dielectric function can be written as

$$\varepsilon^{-1}(\mathbf{q}, \mathbf{q}'|\omega) = (2\pi)^2\delta(\mathbf{Q} - \mathbf{Q}')\varepsilon^{-1}(q_z, q_z'; Q|\omega), \tag{3.1}$$

where $\mathbf{Q}$ and q_z are the components of the wave vector, parallel to and normal to the surface, respectively.

A. Nondispersive solid

As a simple case, we consider a model of a nondispersive semi-infinite solid with an abrupt surface. The dielectric function for this model can easily be obtained by calculating the potential induced by a pointlike charge near the surface and comparing the result with the definition (2.21). This yields

$$\varepsilon^{-1}(k, k'; Q|\omega) = 2\pi\delta(k - k') + \beta(\omega)\frac{i}{k - k' + i0} + [\sigma(\omega) - \beta(\omega)]\frac{1}{Q - ik} + \sigma(\omega)\frac{1}{Q + ik}, \tag{3.2}$$

where the δ-function term corresponds to the external field part of the total induced potential, and the bulk and surface scattering functions have been defined as

$$\beta(\omega)=\frac{1}{\epsilon(\omega)}-1, \tag{3.3}$$

$$\sigma(\omega)=\frac{2}{\epsilon(\omega)+1}-1. \tag{3.4}$$

The inelastic-scattering function (2.20) for this model is

$$W_{\mathbf{k}'\mathbf{k}}(z)=\frac{8\pi e^2}{\hbar q^2}\theta(\epsilon_k-\epsilon_{k'}) \tag{3.5}$$

$$\times\{b(\epsilon_k-\epsilon_{k'})\theta(-z)[1-F(2|z|q_z,2|z|q_\parallel)]$$

$$+s(\epsilon_k-\epsilon_{k'})F(2|z|q_z,2|z|q_\parallel)\},$$

where $\mathbf{q}\equiv\mathbf{k}-\mathbf{k}'$, and

$$F(p_z,p_\parallel)=e^{-p_\parallel}\left[\cos(p_z)+\frac{p_\parallel}{p_z}\sin(p_z)\right], \tag{3.6}$$

$$b(\omega)=-\operatorname{Im}\beta(\omega),$$

$$s(\omega)=-\operatorname{Im}\sigma(\omega).$$

It is seen that the scattering function consists of two separate contributions. The first term, which contains the function *b*, is zero at the surface and increases exponentially to its limiting bulk value as $z\rightarrow-\infty$. The other term, which contains the function *s*, is maximal at the surface and decreases exponentially with the distance from the surface. The inelastic scattering of the electrons in the bulk of the solid ($z\rightarrow-\infty$) are due only to interaction with bulk plasmons, as described by the function *b*. Near the surface the interaction with surface plasmons (described by the function *s*) plays an important role. Precisely at the surface and outside the solid ($z\geqslant 0$), only interaction with surface plasmons leads to electron scattering. The interaction with surface plasmons are present at both sides of the surface and it is symmetrical with respect to surface reflection.

It is interesting to note that the surface part of the scattering function (3.5), besides being exponentially damped with increasing distance from the surface, has an oscillatory behavior with a characteristic wavelength

$$\lambda_{\mathrm{osc}}=\pi/q_z. \tag{3.7}$$

The physical meaning of these oscillations can be understood as follows. The surface part of the scattering results from the interaction of the electron with its own image near the surface. We can imagine the scattering process as a simultaneous exchange of energy of both the electron and its image with an effective wave of charge fluctuations of the solid (see Fig. 1). Both the electron and the image transfer an amount of momentum $\Delta k=q_z$ to the wave and this process is most effective when a resonance condition is satisfied. This implies that the distance between the electron and its image should equal an integer number of wavelengths. But this is exactly the condition (3.7). Consequently the oscillatory behavior of the surface part of the scattering function can be explained as this resonance process.

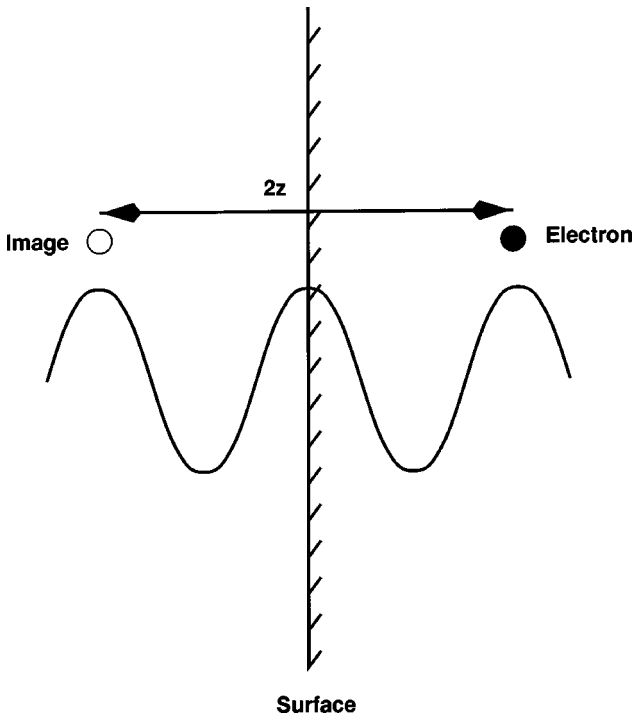

FIG. 1. Resonant interaction between the electron and its image (see text). The scattering is enhanced if the distance between the electron and the image contains an integer number of wavelengths of the effective wave of charge-density fluctuations excited during the scattering process.

For the present model it is relatively easy to obtain an analytic expression for the DIMFP for electron transport along the surface normal. By substituting Eq. (3.5) into Eq. (2.22) we obtain

$$K(E,z,\phi=0;\hbar\omega)$$

$$=\frac{\theta(\omega)}{\pi a_0 E}\{\theta(-z)b(\omega)[J_1(\beta)-J_2(\beta,\alpha)]$$

$$+s(\omega)J_2(\beta,\alpha)\}, \tag{3.8}$$

$$\beta=\sqrt{E/(E-\hbar\omega)},$$

$$\alpha=2|z|\sqrt{2m(E-\hbar\omega)/\hbar^2},$$

where ϕ is the angle between the surface normal and the direction of the electron's path, a_0 is the Bohr radius, and

$$J_1(\beta)=\ln\left|\frac{\beta+1}{\beta-1}\right|, \tag{3.9}$$

$$J_2(\beta,\alpha)=\beta\int_{-1}^{1}dx\frac{F[\alpha(x-\beta),\ \alpha\sqrt{1-x^2}]}{\beta^2-2\beta x+1}. \tag{3.10}$$

The integral (3.10) can be evaluated and expressed by means of exponential integrals of the first kind. However, the ex-

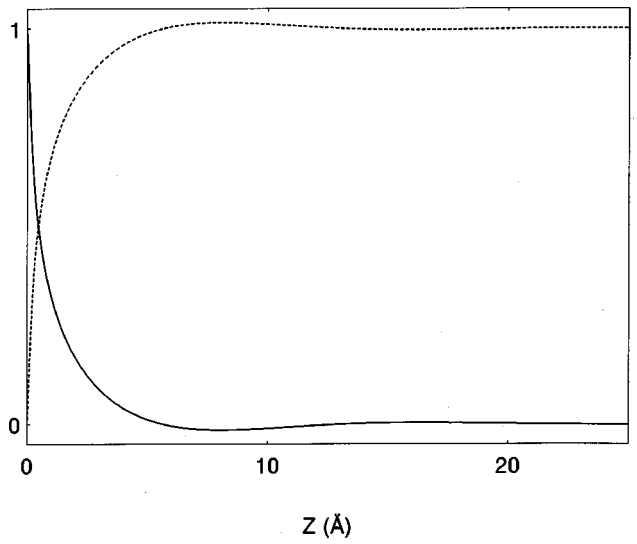

FIG. 2. Depth dependence of the bulk (dotted line) and surface (solid line) components of the scattering function given by Eq. (3.8). The model calculations for electron transport normal to the surface are performed for a nondispersive solid with an abrupt surface. The parameter values of α and β used in the calculation correspond to an electron energy $E=175$ eV and an energy loss $\hbar\omega=10$ eV.

pression is quite complicated and we omit it here. We just note that the usual approximations of replacing

$$\delta(\epsilon_k-\epsilon_{\mathbf{k}-\mathbf{q}}-\omega)\approx\delta(\omega-\mathbf{v_k q}) \tag{3.11}$$

in Eq. (2.22), and taking the recoil effect into account by limiting the range of integration over q by the condition

$$q_-^2\leqslant q^2\leqslant q_+^2\,, \tag{3.12}$$

$$q_\pm=\sqrt{2m/\hbar^2}[\sqrt{E}\pm\sqrt{E-\hbar\omega}],$$

work fairly well for high electron energies.

Figure 2 illustrates the forms of the functions $J_2(\beta,\alpha)/J_1(\beta)$ and $1-J_2(\beta,\alpha)/J_1(\beta)$. These functions represent the depth dependencies of the surface and bulk parts of the inelastic-scattering function, as described by the functions s and b. The relative probability of scattering by surface plasmons decreases from its maximal value at the surface to a vanishing value in the bulk. The relative probability of inelastic scattering on bulk plasmons is zero at the surface and increases asymptotically to the bulk value, as expected. The functions have an oscillatory behavior with a period $1/2q_-$ corresponding to the cutoff of the minimum momentum transfer from the electron-image pair to the solid.

Quite naturally, the DIMFP can be split into bulk and surface parts as

$$K(E,z,\phi;\hbar\omega)=\theta(-z)K_{\mathrm{B}}(E;\hbar\omega)+K_{\mathrm{S}}(E,z,\phi;\hbar\omega), \tag{3.13}$$

where K_{B} is the only term appearing in the transport equations when surface effects are neglected. In a situation where the effective penetration depth of the electron into the solid is large compared to the width of the surface scattering layer, it appears useful to introduce an integral parameter to characterize the effect of the surface. In Ref. 2 a differential surface excitation parameter was introduced as

$$P_{\mathrm{S}}(E,\phi;\hbar\omega)=\int_{-\infty}^{\infty}\frac{dz}{\cos\phi}K_{\mathrm{S}}(E,z,\phi;\hbar\omega). \tag{3.14}$$

Additionally, a surface excitation parameter for an electron crossing the surface is defined as[2]

$$P_{\mathrm{S}}(E,\phi)=\int_0^E P_{\mathrm{S}}(E,\phi;\hbar\omega)d(\hbar\omega). \tag{3.15}$$

In the present simple model for a nondispersive solid, the differential surface excitation parameter can easily be calculated by use of the approximation Eq. (3.11) and by neglect of the recoil effect. Substitution of Eq. (3.5) into Eq. (2.22) and performing the integration in Eq. (3.14) leads to

$$P_{\mathrm{S}}(E,\phi;\hbar\omega)=\frac{e^2}{2\hbar^2\omega v\cos\phi}[2s(\omega)-b(\omega)], \tag{3.16}$$

where v is the velocity of the electron. Since it follows from Eqs. (3.3)–(3.5) that

$$2s(\omega)-b(\omega)=\mathrm{Im}\left[\frac{[1-\epsilon(\omega)]^2}{\epsilon(\omega)[1+\epsilon(\omega)]}\right], \tag{3.17}$$

we find that Eq. (3.16) reproduces the result recently obtained by Chen and Chen[22] using a different surface scattering function; this is discussed later in Sec. V. Note that the first term in Eq. (3.16) corresponds to the scattering on surface excitations while the second term represents the decrease of scattering on bulk excitations near the surface.

If we use the dielectric function for the free-electron gas

$$\epsilon(\omega)=1-\frac{\omega_0^2}{(\omega+i\eta)^2},\quad \eta\to 0, \tag{3.18}$$

then we immediately find that

$$b(\omega)=\frac{\pi\omega_0}{2}[\delta(\omega-\omega_0)-\delta(\omega+\omega_0)], \tag{3.19}$$

$$s(\omega)=\frac{\pi\omega_s}{2}[\delta(\omega-\omega_s)-\delta(\omega+\omega_s)], \tag{3.20}$$

$$\omega_s=\omega_0/\sqrt{2}.$$

The integration in Eq. (3.15) can now easily be performed with the result

$$P_{\mathrm{S}}(E,\phi)=\frac{1}{\cos\phi}[Q_{\mathrm{S}}-Q_{\mathrm{B}}], \tag{3.21}$$

$$Q_{\mathrm{S}}=2Q_{\mathrm{B}}=\frac{\pi e^2}{2\hbar v}.$$

where Q_{S} is the probability that the electron will excite a surface excitation while passing through the surface along the normal direction. This result is well known.[13,29,30]

B. Surface models of dispersive solids

It is commonly recognized that the k dependence of the dielectric function $\varepsilon(\mathbf{k},\omega)$ must be taken into account in order to provide a proper quantitative description of the effects of bulk scattering on the electron energy-loss spectra. Fortunately, for calculations of solid parameters like the DIMFP, only the behavior at small k values plays a major role and quite simple models can be employed for the dielectric function. The problem becomes more complicated when the effects of the surface are considered. One needs to choose an appropriate model for the generalized dielectric function (3.1), which includes information both on the bulk and on the surface excitations of the actual solid. During the past decades considerable progress has been achieved in developing a quantum-mechanical theory of surface plasmon excitations and the dielectric properties of solid surfaces; Ref. 31 mention just a few of these works. However, these results are difficult to use in practical electron spectroscopy applications since they require excessive calculations. Therefore, a number of semiempirical surface models have been developed.[23,19,18,22,21] We will use two of these models for a calculation of the surface scattering function based on the theory presented above.

The first model, known as the specular reflection surface model, was suggested in Ref. 23. The generalized dielectric function for this model has the form (see the Appendix for a derivation)

$$\begin{aligned}\varepsilon^{-1}(z,z';Q|\omega) &= \delta(z-z')+\theta(-z)\,\theta(-z')\\ &\times[\beta(z-z',Q;\omega)+\beta(z+z',Q;\omega)]\\ &+\theta(-z')\frac{2\beta(z',Q;\omega)}{2+\tilde{\beta}(Q,\omega)}\\ &\times[\theta(z)e^{-Qz}-\theta(-z)\\ &\times\{e^{Qz}+\tilde{\beta}(z,Q;\omega)\}],\end{aligned} \tag{3.22}$$

where we have used the mixed $(z,\mathbf{Q})$ representation defined by

$$f(z,\mathbf{Q})=\int_{-\infty}^{\infty}\frac{dq_z}{2\pi}e^{iq_z z}f(\mathbf{q}) \tag{3.23}$$

and, similar to Eq. (3.3),

$$\beta(z',Q;\omega)\equiv\int_{-\infty}^{\infty}\frac{dq_z}{2\pi}\left[\frac{1}{\varepsilon(\mathbf{q},\omega)}-1\right]e^{iq_z z}. \tag{3.24}$$

Also

$$\tilde{\beta}(z,\mathbf{Q},\omega)\equiv\frac{Q}{\pi}\int_{-\infty}^{\infty}dq_z\frac{\beta(\mathbf{q},\omega)e^{iq_z z}}{q^2} \tag{3.25}$$

and

$$\tilde{\beta}(\mathbf{Q},\omega)\equiv\tilde{\beta}(z=0,\mathbf{Q},\omega). \tag{3.26}$$

The second model, which can be found in Ref. 22, gives the following generalized dielectric function:

$$\begin{aligned}\varepsilon^{-1}(z,z';Q|\omega) &= \delta(z-z')+\theta(-z)\beta(z-z',Q;\omega)\\ &+\frac{\beta(z',Q;\omega)}{2+\tilde{\beta}(Q,\omega)}[\theta(z)e^{-Qz}-\theta(-z)\\ &\times\{e^{Qz}+\tilde{\beta}(z,Q;\omega)\}].\end{aligned} \tag{3.27}$$

For nondispersive models with $\varepsilon(\mathbf{q},\omega)=\epsilon(\omega)$, both Eqs. (3.22) and (3.27) simplify to

$$\begin{aligned}\varepsilon^{-1}(z,z';Q|\omega) &= \delta(z-z')+\beta(\omega)\,\theta(-z)\\ &\times[\delta(z-z')-\delta(z')e^{Qz}]\\ &+\sigma(\omega)\,\delta(z')e^{-Q|z|},\end{aligned} \tag{3.28}$$

which conforms with the result obtained in Ref. 32 and after Fourier transformation coincides with Eq. (3.2).

In order to see how the choice of surface model can affect the results of a simulation of electron scattering in the surface region we performed some calculations. We chose Al as an example since it is one of the simplest real materials. As a model function for the bulk dielectric function we took[1,33,20]

$$\varepsilon^{-1}(\mathbf{q},\omega)=1+\frac{\omega_0^2}{(\omega+i\gamma)^2-\omega(\mathbf{q})^2}, \tag{3.29}$$

$$\omega(\mathbf{q})=\omega_0+\hbar q^2/2m, \tag{3.30}$$

which corresponds to a single plasmon mode with damping γ and a free-electron dispersion law. We used the parameters values $\gamma=0.54$ eV (Ref. 34) and $\omega_0=15.0$ eV.

Figure 3 displays the results of a calculation of the DIMFP defined by Eq. (2.22) for the case of electron transport along the normal to the surface ($\phi=0$). The energy of the electron is $E_0=175$ eV. The calculation was performed for the two surface models defined by Eqs. (3.22) and (3.27). As expected, the surface-plasmon peak located near the surface ($z=0$) is observed with an energy about 10 eV. The bulk scattering for $z\leqslant -15$ Å is determined by the bulk plasmon peak with an energy about 15 eV and the shoulder extending to the region of higher energies due to bulk plasmon dispersion. There is a clearly observed difference between the results of the two surface models, e.g., more prominent oscillations of the differential inverse inelastic mean free path is found for the specular reflection surface model [Fig. 3(a)]. The presence of oscillations for both of the two dispersive models indicates that the oscillations are not just a property of the nondispersive solid model. One might expect, however, that the effect of the resonance interaction of the electron with its image will be degraded more seriously when nonabruptness of the surface is taken into account.

Figure 4 displays the differential surface excitation parameter, defined in Eq. (3.14), calculated for the same two models and with the same parameter values as in Fig. 3. The difference between the two models is again rather evident and, as one can see, concerns mainly the shape and position of the surface scattering peak. For both models the surface

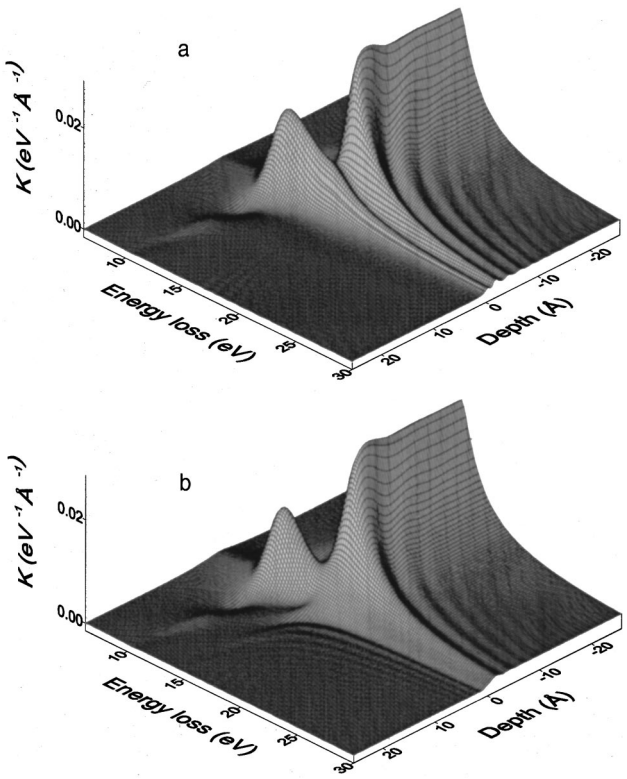

FIG. 3. Differential inverse inelastic mean-free-path $K(E_0,z,\phi=0;\hbar\omega)$ for Al at electron energy $E_0=175$ eV calculated using (a) the specular reflection model [Eq. (3.22)], (b) the model of Ref. 22 [Eq. (3.27)]. Equation (3.29) was used for the calculation of the bulk dielectric function with $\omega_0=15.0$ eV and $\gamma=0.54$ eV.

peak is positioned at higher energies than would be expected from the nondispersive value $\omega_0/\sqrt{2}=10.6$ eV. The surface peak in the specular reflection model is shifted to higher energies than the corresponding peak in the model described by Eq. (3.27). The positive shift of the surface peak originates from the dispersion law of the surface plasmon, which

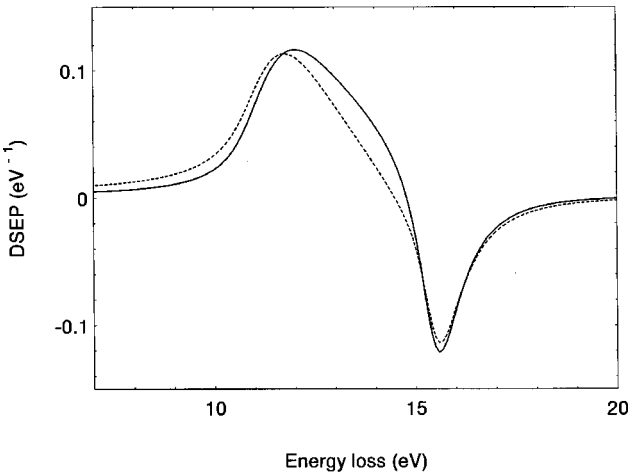

FIG. 4. Differential surface excitation parameter $P_S(E_0,\phi=0;\hbar\omega)$ for Al at electron energy $E_0=175$ eV. Solid line: specular reflection model [Eq. (3.22)]. Dotted line: the model of Ref. 22 [Eq. (3.27)].

for both of the two considered models, is determined by the equation

$$\tilde{\beta}(Q,\omega)=-2 \tag{3.31}$$

and which is positive for small Q values.[23] This behavior is in contradiction with the known experimental data[35] from which a negative dispersion law for the surface plasmons follows and which indicates, as first shown in Ref. 36, that the surface charge density profile plays an important role, so that the abruptness of the surface will be a poor approximation.

The conclusion is that data obtained by high-energy electron scattering experiments are sensitive to quite subtle properties of the surface when the surface effects on the electron transport can be parametrized by either the DIMFP or the differential surface excitation parameter. Thus one might hope to obtain useful information about the surface from such experiments. In the next section we consider possible ways to include the effects of surface scattering in a description of REELS and XPS/AES data.

IV. EFFECTS OF SURFACE SCATTERING IN REELS AND XPS/AES

We start by considering a particularly simple case, the so-called straight-line approximation (SLA), where both the elastic scattering and the angular deflection of the electron due to inelastic scattering are neglected. By exploiting the symmetry of the surface, we can write the stationary form of the Boltzmann's equation (2.17), in a source free region, as

$$\left[\cos\phi\frac{\partial}{\partial z}+\lambda_i(E,z,\phi)^{-1}\right]\rho(E,z,\phi) = \int_{-\infty}^{\infty}dE'K(E',z,\phi;E'-E)\rho(E',z,\phi), \tag{4.1}$$

where $\rho(E,z,\phi)$ is the density of electrons with energy E at depth z and with a path direction (velocity of the electron) given by the polar angle ϕ. The inelastic mean free path $\lambda_i(E,z,\phi)$ is defined by

$$\lambda_i(E,z,\phi)^{-1}\equiv\int_{-\infty}^{\infty}d\epsilon K(E,z,\phi;\epsilon). \tag{4.2}$$

If the energy loss due to inelastic scattering is much smaller than the total kinetic energy of the electrons then the solution to Eq. (4.1) can be written as

$$\rho(E,z,\phi)=\int_{-\infty}^{\infty}dE'G(E,z,z_0,\phi;E'-E)\rho(E',z_0,\phi), \tag{4.3}$$

where the energy loss for any paths from z_0 to z is equal to

$$G(E,z,z_0,\phi;\epsilon)=\int_{-\infty}^{\infty}\frac{ds}{2\pi}\exp\left[is\epsilon - \int_{z_0}^{z}\frac{dz'}{\cos\phi}\Sigma(E,z',\phi;s)\right] \quad (4.4)$$

with

$$\Sigma(E,z,\phi;s)=\int_{-\infty}^{\infty}d\epsilon K(E,z,\phi;\epsilon)[1-e^{-is\epsilon}]. \quad (4.5)$$

Equations (4.3)–(4.5) generalize Landau's formula[14] to spatially inhomogeneous scattering functions.

We will now try to derive simple formulas that can be used for analysis of REELS and XPS or AES spectra and include the effects of surface scattering. In order to do so, we assume that the transport of the electrons through the surface layer can be treated by the straight-line approximation. This assumption requires that the effective width of the surface layer must be sufficiently smaller than the transport mean-free-path for elastic scattering. This requirement is usually fulfilled for electron energies above 50 eV, which are commonly used in REELS and XPS/AES except for grazing angle values ($\phi\simeq 90°$). Under the same conditions, we may also assume that the major part of the electrons observed in the recorded spectra cross the surface layer completely, i.e., we neglect electrons originating from within the surface layer in the case of XPS/AES and electrons backscattered within the surface layer in the case of REELS.

The electrons observed in an experiment are those leaving the surface. The observed spectrum can therefore be represented as

$$\begin{aligned}S(E,\phi)&=\cos\phi\ \ \rho(E,z=\infty,\phi)\\&=\cos\phi\int_{-\infty}^{\infty}dE'G(E,\infty,-d,\phi;E'-E)\\&\quad\times\rho(E',-d,\phi),\end{aligned} \quad (4.6)$$

where the value of $z_0=-d$ should be larger than the width of the surface but small enough that the SLA can be used within the layer $-d<z<0$. According to Eq. (3.13) we may split the function (4.5) into a bulk and a surface part as

$$\Sigma(E,z,\phi;s)=\Sigma_S(E,z,\phi;s)+\theta(-z)\Sigma_B(E;s) \quad (4.7)$$

with

$$\Sigma_S(E,z,\phi;s)=\int_{-\infty}^{\infty}d\epsilon K_S(E,z,\phi;\epsilon)[1-e^{-is\epsilon}] \quad (4.8)$$

and

$$\Sigma_B(E;s)=\int_{-\infty}^{\infty}d\epsilon K_B(E;\epsilon)[1-e^{-is\epsilon}]. \quad (4.9)$$

By use of Eq. (4.7) the integral term in the exponent of Eq. (4.4) can, for $z=\infty$ and $z_0=-d$, be rewritten as

$$\begin{aligned}\int_{-d}^{\infty}\frac{dz'}{\cos\phi}\Sigma(E,z',\phi;s)&=\int_{-d}^{\infty}\frac{dz'}{\cos\phi}\Sigma_S(E,z',\phi;s)+\int_{-d}^{0}\frac{dz'}{\cos\phi}\Sigma_B(E;s)\\&\simeq\int_{-\infty}^{\infty}\frac{dz'}{\cos\phi}\Sigma_S(E,z',\phi;s)+\frac{d}{\cos\phi}\Sigma_B(E;s).\end{aligned} \quad (4.10)$$

The energy-loss function in Eq. (4.6) can then be written as the convolution

$$G(E,\infty,-d,\phi;\epsilon)=\int_{-\infty}^{\infty}d\epsilon' G_S(E,\phi;\epsilon')\times G_L\left(E,\frac{d}{\cos\phi};\epsilon-\epsilon'\right), \quad (4.11)$$

where

$$G_L(E,R;\epsilon)=\int_{-\infty}^{\infty}\frac{ds}{2\pi}\exp[is\epsilon-R\Sigma_B(E;s)] \quad (4.12)$$

is Landau's energy loss function,[14] and

$$G_S(E,\phi;\epsilon)=\int_{-\infty}^{\infty}\frac{ds}{2\pi}\exp[is\epsilon-\Xi(E,\phi;s)] \quad (4.13)$$

with

$$\Xi(E,\phi;s)=\int_{-\infty}^{\infty}d\epsilon P_S(E,\phi;\epsilon)[1-e^{-is\epsilon}] \quad (4.14)$$

is the surface loss function that can be found in Refs. 37. The definition (3.14) of the differential surface excitation parameter (P_S) was used to obtain Eq. (4.14). Since we have assumed that the value of d is small enough that the SLA can be applied, we find that

$$\rho_0(E,z=0;\phi)=\int_{-\infty}^{\infty}dE'G_L\left(E,\frac{d}{\cos\phi};E'-E\right)\times\rho(E',-d,\phi) \quad (4.15)$$

is the density of outgoing electrons at $z=0$, which would result if surface scattering was absent. By inserting Eq. (4.11) into Eq. (4.6) and using the Eq. (4.15) we finally obtain the expression

$$S(E,\phi)=\int_{-\infty}^{\infty}dE'G_S(E,\phi;E'-E)S_0(E',\phi), \quad (4.16)$$

which relates the actually observed spectrum (S) with the spectrum (S_0) of a ''nonperturbed'' solid, i.e., one for which the effect of surface scattering is neglected. This relation has recently been obtained by Chen and Chen[22] who applied it to an analysis of XPS spectra with surface scattering effects taken into account.

Similar arguments can be used to derive the modifications of the spectrum of incident electrons caused by surface scattering. The effective electron density at $z=0$ corresponding to a ''nonperturbed'' solid is related to the density of incident electrons by

$$\rho_0(E,z=0;\phi)=\int_{-\infty}^{\infty} dE' G_S(E,\phi;E'-E)\rho(E',z=\infty,\phi). \tag{4.17}$$

Combining Eqs. (4.16) and (4.17) yields a relation between the reflected electron energy-loss spectrum observed experimentally and the corresponding spectrum calculated with surface scattering neglected. This relation can be written as

$$R(E_0,\phi_0;E,\phi)=\int_{-\infty}^{\infty} dE' G_{SS}(E_0,\phi_0,\phi;E'-E) \times R_0(E_0,\phi_0;E',\phi), \tag{4.18}$$

where $R(E_0,\phi_0;E,\phi)$ is the conditional probability distribution for an incident electron with energy E_0 and direction ϕ_0 to be reflected in the direction ϕ with energy E; the corresponding value for the ''nonperturbed'' solid is denoted R_0. As before, we neglect the dependence of the total electron energy in comparison with that of the energy loss. The ''nonperturbed'' reflection spectrum is modified through a convolution with the surface double-loss function

$$G_{SS}(E_0,\phi_0,\phi;\epsilon)=\int_{-\infty}^{\infty} d\epsilon' G_S(E_0,\phi_0;\epsilon')G_S(E_0,\phi;\epsilon-\epsilon') = \int_{-\infty}^{\infty}\frac{ds}{2\pi}\exp[is\epsilon-\Xi(E_0,\phi;s) - \Xi(E_0,\phi_0;s)]. \tag{4.19}$$

Equations (4.16) and (4.18) provide a correction procedure for model spectra calculated without consideration of the effects of surfacing scattering. The corrected spectra, that include the effect of surface scattering, are obtained simply by a convolution with the appropriate surface loss function. Since bulk and surface properties are completely separated in these formulas it may be possible to determine the surface properties, expressed by the differential surface excitation parameter $P_S(E,\phi;\epsilon)$, from experimental data by using the ''nonperturbed'' spectra as references.

We now outline an algorithm for retrieving the surface loss function from experimental REELS spectra. We suppose for simplicity that the bulk differential inverse inelastic mean free path $K_B(\epsilon)$ has been determined from other sources and that the corresponding ''nonperturbed'' energy loss spectrum $R_0(\epsilon)$ can be calculated by a theoretical model, e.g., the P_1 approximation[7] or the transport approximation,[38,10,11] which are known to give more or less reliable results. For brevity we omit the dependence on the energy and direction of the incident electron, leaving only the energy loss ϵ as variable. By defining s as the Fourier transformed variable corresponding to the energy variable ϵ we can, quite generally, write the Fourier transform of the ''nonperturbed'' energy loss spectrum as

$$R_0(s)=R_0+R_1K_B(s)+R_2K_B^2(s)+\cdots=R_0+Q_0(s), \tag{4.20}$$

where R_0 represents the elastic reflection peak and $Q_0(s)$ is the inelastic energy-loss spectrum consisting of one-, two- and more inelastic scattering peaks (represented by R_1, R_2, etc.). The experimental spectrum can also be represented as a combination of the elastic peak and the inelastic energy loss part as

$$R(s)=R+Q(s), \tag{4.21}$$

where the inelastic part $Q(s)$ is now a mixture of multiple bulk and surface scattering peaks. Similarly, the surface loss function may be split into a combination of an ''elastic'' peak and an inelastic-scattering part as

$$G_{SS}(s)=G_0+G_{inel}(s) \tag{4.22}$$

with

$$G_0=\exp[-P_S(E,\phi)-P_S(E,\phi_0)], \tag{4.23}$$

$$G_{inel}(s)=G_0\sum_{k=1}^{\infty}\frac{1}{k!}[P_S(E,\phi;s)+P_S(E,\phi_0;s)]^k. \tag{4.24}$$

Fourier transformation of Eq. (4.18) gives the simple relation

$$R(s)=G_{SS}(s)R_0(s), \tag{4.25}$$

which after insertion of Eqs. (4.20)–(4.22) and separation into a constant part and one that depends on the variable s yields

$$G_0=R/R_0 \tag{4.26}$$

and

$$G_{inel}(s)=A(s)-B(s)G_{inel}(s), \tag{4.27}$$

where we have defined

$$A(s)=\frac{Q(s)}{R_0}-\frac{RQ_0(s)}{R_0^2}, \tag{4.28}$$

$$B(s)=\frac{Q_0(s)}{R_0}. \tag{4.29}$$

Since all the energy-loss functions $Q(\epsilon)$, $Q_0(\epsilon)$, and $G_{inel}(\epsilon)$ have nonzero values only for $\epsilon>0$, Eq. (4.27) transformed into the energy variables has the form

$$G_{inel}(\epsilon)=A(\epsilon)-\int_0^{\epsilon} d\epsilon' B(\epsilon-\epsilon')G_{inel}(\epsilon'). \tag{4.30}$$

This integral equation for $G_{inel}(\epsilon)$ can be solved recursively, e.g., by the procedure proposed in Ref. 39. After G_0 and $G_{inel}(\epsilon)$ are found, the values of $P_S(E,\phi)+P_S(E,\phi_0)$ and $P_S(E,\phi;\epsilon)+P_S(E,\phi_0;\epsilon)$ can be obtained from Eqs. (4.23) and (4.24). For $\phi=\phi_0$ this would give us both the differen-

tial surface excitation parameter and the surface excitation parameter of the surface scattering. A consistency check of the procedure is provided by the relation (3.15).

V. COMPARISON WITH STOPPING-POWER METHODS

In this section we compare the present results, obtained by a quantum-mechanical derivation of a localized Boltzmann's equation, with those based on a calculation of the stopping power.[13,19,20,22,21] In the stopping-power approach, it is assumed that the fast electron moves along a classical trajectory and the effect of the medium is calculated as the force acting upon the electron due to the induced potential of the medium caused by the field of the moving electron. Let us consider an electron moving along a straight line with velocity **v**, for which the charge density

$$\rho(\mathbf{r},t)=e\,\delta(\mathbf{r}-\mathbf{r}_0-\mathbf{v}t), \tag{5.1}$$

and its Fourier transform

$$\rho(\mathbf{q},\omega)=e\,\delta(\omega-\mathbf{v}\mathbf{q})e^{-i\mathbf{q}\mathbf{r}_0}. \tag{5.2}$$

The direct field of the moving charge is then

$$\phi_{\rm ext}(\mathbf{q},\omega)=\frac{8\pi^2 e}{q^2}\,\delta(\omega-\mathbf{v}\mathbf{q})e^{-i\mathbf{q}\mathbf{r}_0}. \tag{5.3}$$

The induced potential of the medium can be expressed in items of the generalized dielectric function, defined by Eq. (2.21), as

$$\phi_{\rm ind}(\mathbf{r},t)=8\pi^2 e\int\frac{d\omega}{2\pi}\int\frac{d^3q}{(2\pi)^3}\int\frac{d^3q'}{(2\pi)^3}\,\frac{\delta(\omega-\mathbf{v}\mathbf{q}')}{q'^2}\times[\varepsilon^{-1}(\mathbf{q},\mathbf{q}'|\omega)-(2\pi)^3\delta(\mathbf{q}-\mathbf{q}')]e^{i\mathbf{q}\mathbf{r}-i\mathbf{q}'\mathbf{r}_0-i\omega t}. \tag{5.4}$$

The spatially dependent stopping power can then be calculated from Eq. (5.4) as[19,22]

$$-\frac{dW}{dS}=-\frac{e}{v}\left[\frac{\partial\phi_{\rm ind}(\mathbf{r},t)}{\partial t}\right]_{\mathbf{r}=\mathbf{r}_0+\mathbf{v}t} \tag{5.5}$$

with the result

$$-\frac{dW}{dS}=-\frac{4i\pi e^2}{v}\int\omega d\omega\int\frac{d^3q}{(2\pi)^3}\int\frac{d^3q'}{(2\pi)^3}\,\frac{\delta(\omega-\mathbf{v}\mathbf{q}')}{q'^2}\times[\varepsilon^{-1}(\mathbf{q},\mathbf{q}'|\omega)-(2\pi)^3\delta(\mathbf{q}-\mathbf{q}')]e^{i(\mathbf{q}-\mathbf{q}')\mathbf{r}}. \tag{5.6}$$

In the stopping-power approach, the energy-loss function is then obtained by use of the relation between the stopping power and the DIMFP

$$-\frac{dW}{dS}=\int_0^\infty(\hbar\omega)K(\hbar\omega)d(\hbar\omega). \tag{5.7}$$

The quantum-mechanical expression for the stopping power, which follows from our derivation of the differential inverse inelastic mean free path given by Eq. (2.23) and the relation (5.7), is

$$-\frac{dW}{dS}=-\frac{4i\pi e^2}{v}\int\omega d\omega\int\frac{d^3q}{(2\pi)^3}\int\frac{d^3q'}{(2\pi)^3}\times\frac{\delta(\omega-\mathbf{v}(\mathbf{q}+\mathbf{q}')/2)}{q'^2}[\varepsilon^{-1}(\mathbf{q},\mathbf{q}'|\omega)-(2\pi)^3\delta(\mathbf{q}-\mathbf{q}')]e^{i(\mathbf{q}-\mathbf{q}')\mathbf{r}}, \tag{5.8}$$

where we have used the property $\varepsilon^{-1}(\mathbf{q},\mathbf{q}'|\omega)=[\varepsilon^{-1}(-\mathbf{q},-\mathbf{q}'|-\omega)]^*$ and the high-energy approximation given by Eq. (3.11).

It is instructive to compare the above classical and quantum-mechanical expressions for the stopping power by use of the coordinate representation for the dielectric function. If we introduce the definition

$$\beta(\mathbf{r},\mathbf{r}'|\tau)=\int\frac{d\omega}{2\pi}\int\frac{d^3q}{(2\pi)^3}\int\frac{d^3q'}{(2\pi)^3}[\varepsilon^{-1}(\mathbf{q},\mathbf{q}'|\omega)-(2\pi)^3\delta(\mathbf{q}-\mathbf{q}')]\exp(i\mathbf{q}\mathbf{r}-i\mathbf{q}'\mathbf{r}'-i\omega\tau) \tag{5.9}$$

then the classical Eq. (5.6) can be written as

$$-\frac{dW}{dS}=\frac{e^2}{v}\int d^3r'\int d\tau\dot{\beta}(\mathbf{r},\mathbf{r}'|\tau)\frac{1}{|\mathbf{r}-\mathbf{v}\tau-\mathbf{r}'|}, \tag{5.10}$$

while the quantum-mechanical Eq. (5.8) is transformed into

$$-\frac{dW}{dS}=\frac{e^2}{v}\int d^3r'\int d\tau\dot{\beta}\left(\mathbf{r}+\frac{\mathbf{v}\tau}{2},\mathbf{r}'+\frac{\mathbf{v}\tau}{2}\middle|\tau\right)\frac{1}{|\mathbf{r}-\mathbf{v}\tau-\mathbf{r}'|}. \tag{5.11}$$

As usual, $\dot{\beta}$ denotes the time derivative of the function defined by Eq. (5.9). The physical origin of the difference between the classical and the quantum-mechanical expressions for the stopping power is clearly seen from Eqs. (5.10) and (5.11). In the classical treatment, the stopping power at point **r** results from the interaction of the electron at this point with the polarization of the medium induced by the same electron; the electron is described as a pointlike particle moving along a classical trajectory. In our quantum-mechanical treatment of spatially inhomogeneous media, we must compromise between uncertainties in the position and the momentum of the electron. Consequently, instead of a pointlike particle we need a wave packet of finite spatial size. Equation (5.11) for the stopping power takes into account that the medium is polarized beforehand, i.e., by the front of the moving wave packet, as reflected by the change of the second argument in the dielectric response function from $\mathbf{r}'$ to $\mathbf{r}'+\mathbf{v}\tau/2$. Similarly, the first argument of $\dot{\beta}$ is $\mathbf{r}+\mathbf{v}\tau/2$ rather than **r**, which indicates that the front of the packet is first to interact with the polarization of the medium.

A comparison of Eqs. (5.6) and (5.8) shows that there are two situations where the results obtained from a calculation of the stopping power for classically moving electrons and from the Boltzmann equation are equivalent. The first case occurs for spatially homogeneous media where Eq. (2.24) holds, and $\mathbf{q}=\mathbf{q}'$. The equivalence of the quantum-mechanical and the quasiclassical treatments for homogeneous media has previously been demonstrated by Ritchie.[13,28] Another case is found by integrating Eqs. (5.6) and (5.8) over the spatial variable. The integration converts the exponential function $\exp[i(\mathbf{q}-\mathbf{q}')\mathbf{r}]$ into the delta-function $\delta(\mathbf{q}-\mathbf{q}')$ and thus again we have $\mathbf{q}=\mathbf{q}'$. This means that the two approaches are equivalent with respect to calculations of the energy loss averaged over the electron path. This, for example, is of interest for calculations of the differential surface excitation parameter, Eq. (3.14), and the surface excitation parameter, Eq. (3.15), and we have already demonstrated the equivalence of the differential surface excitation parameter calculated by our approach, Eq. (3.16), with the corresponding result, recently obtained by Chen and Chen,[22] by a stopping-power calculation. For these two situations the localization of the electron, assumed by using a classical trajectory, is not essential for the final result. For a homogeneous medium the scattering properties are spatially independent (the stopping power given by Eq. (5.6) does not depend on $\mathbf{r}$ for $\mathbf{q}=\mathbf{q}'$) and in the latter case an average over the trajectory is performed.

The difference between the stopping-power approach and the Boltzmann's equation approach becomes essential when the spatial structure of the scattering function is considered. As an example, we use the expression obtained by Chen and Chen[22] to calculate the differential inverse inelastic mean-free-path for an electron leaving the solid in the normal direction using the nondispersive solid model. The result is

$$K(E,z,\phi=0;\hbar\omega)=\frac{\theta(\omega)}{\pi a_0 E}\{\theta(-z)b(\omega)[J_1-J_2(z)] + s(\omega)(\theta(-z)J_2(z)+\theta(z) \times[J_3(z)-J_2(z)])\}, \tag{5.12}$$

where J_1 is given by Eq. (3.9),

$$J_2(z)=\int_{q_-}^{q_+} dQ\,\frac{Qe^{-2Q|z|}}{Q^2+(\omega/v)^2}, \tag{5.13}$$

$$J_3(z)=2\cos\left(\frac{\omega z}{v}\right)J_2\left(\frac{z}{2}\right), \tag{5.14}$$

and $q_\pm$ is defined in Eq. (3.13). It is easy to see that Eq. (5.12) differs from the corresponding expression obtained by our theory, Eq. (3.8). Figure 5 displays the surface part of the scattering function [the part involving $s(\omega)$] for both expressions. Equation (5.12) is asymmetrical for an electron moving inside and outside of the solid, while our expression, Eq. (3.8), is symmetrical about the surface. Equation (5.12) does produce oscillations outside the solid, although with a wavelength about twice as large as that obtained by our theory, it does not predict oscillations inside the solid.

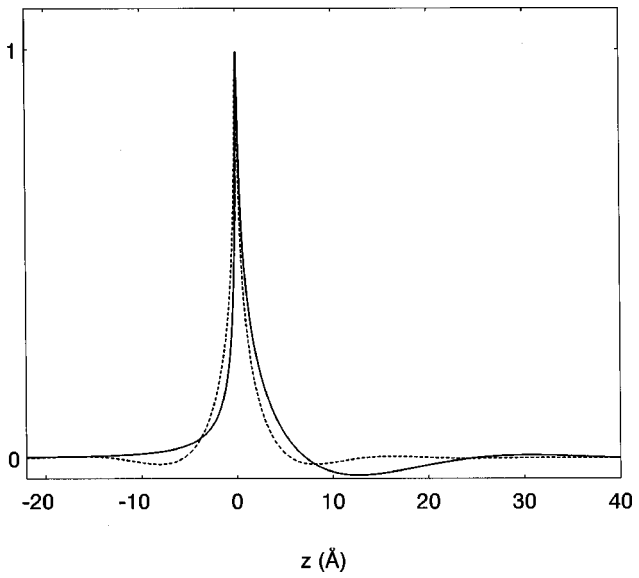

FIG. 5. Depth dependence of the surface part of the DIMFP for an electron leaving the solid in the normal direction. The calculations are performed for the nondispersive solid model with an electron energy $E=175$ eV and energy loss $\hbar\omega=10$ eV. Solid line: calculation using the stopping-power approach. Dotted line: calculation based on the theory presented in the present paper [Eq. (3.8)].

The difference between the spatial dependencies of the scattering function obtained by the two methods can be explained by an internal inconsistency of the problem formulation. Due to the uncertainty principle, an exact specification of the position of the electron, required in the context of a spatially dependent scattering function, leads to an uncertainty of the electron energy and thus to an uncertainty in the definition of the energy-loss function. The local approximation to the quantum Boltzmann's equation, which we introduced above, provides a reasonable compromise between uncertainty in position and energy. Therefore, we believe that the definition of a spatially dependent scattering function in the context of a localized Boltzmann's equation is more appropriate than the one used previously by stopping-power calculations based on a classical trajectory of the electron.

VI. CONCLUSIONS

We have derived a Boltzmann-type transport equation for high-energy electrons interacting with an inhomogeneous solid. The effect of the spatial inhomogeneity on the inelastic scattering of the electrons is described self-consistently by a generalized dielectric function of the solid. A model calculation of the transport properties near the surface was performed. It was found that the spatial dependence of the inelastic-scattering function derived from our description, is significantly different from that obtained from a calculation of the stopping power for electrons moving along classical trajectories. The spatial dependence obtained by the present formalism has an oscillatory behavior near the surface that can be explained as resulting from the resonant interaction of the electron with its image. The two approaches give identical results only when the detailed spatial dependence of the

scattering function is unimportant. This includes calculations of the integrated energy loss of an electron crossing the surface, as expressed by the differential surface excitation parameter. A determination of the differential surface excitation parameter seems to be sufficient for a quantitative description of surface effects in situations where the mean-free-path of the electron exceeds the effective width of the surface layer, e.g., in the high-electron energy limit of REELS and XPS/AES. However, as we have demonstrated, the values of the differential surface excitation parameter is rather sensitive to the surface parameters and the interpretation of experimental data can thus be significantly affected by the choice of surface model. We suggest that an experimental determination of the differential surface excitation parameter could be of interest for understanding the surface properties and for a proper quantification of other experimental results. We have outlined an algorithm that could be useful for estimations of the differential surface excitation parameter from experimental REELS data.

ACKNOWLEDGMENTS

We are grateful to the Danish Natural Science Research Council for the support of KLA.

APPENDIX: GENERALIZED DIELECTRIC FUNCTION IN THE SPECULAR SURFACE MODEL

In this appendix we present a derivation of the inverse generalized dielectric function, defined by Eq. (2.21), for the specular reflection surface model introduced by Ritchie and Marusak.[23] The model assumes that the quasiparticles of the solid are specularly reflected at the inside of the surface. The problem of finding the induced potential of the medium, as a response to an external charge distribution, can be successfully treated by the method of extended pseudomedia.[19,40,41,21] For the geometry described in Sec. III, the total potential in the presence of the external charge can be written as

$$\phi(z,\mathbf{Q};\omega)=\theta(z)\,\phi_+(z,\mathbf{Q};\omega)+\theta(-z)\,\phi_-(z,\mathbf{Q};\omega), \tag{A1}$$

where ϕ_+,ϕ_- are the potentials in the extended pseudovacuum and pseudosolid, respectively, and the transformation of all functions to the variables $(z,\mathbf{Q})$ is defined by Eq. (3.23). The potentials $\phi_\pm$ for the extended pseudomedia are defined by

$$\phi_\pm(\mathbf{q},\omega)=\frac{4\pi}{q^2\varepsilon_\pm(\mathbf{q},\omega)}[\rho_0^\pm(\mathbf{q},\omega)+\sigma_S^\pm(\mathbf{Q},\omega)], \tag{A2}$$

where σ_S is the fictitious surface charge, and ρ_0^+,ρ_0^- are the effective symmetrized charge distributions corresponding to each pseudomedia. These charge distributions are related to the real external charge distribution $\rho_0(\mathbf{q},\omega)$ by

$$\rho_0^\pm(z,\mathbf{Q};\omega)=\theta(z)\rho_0(\pm z,\mathbf{Q};\omega)+\theta(-z)\rho_0(\mp z,\mathbf{Q};\omega). \tag{A3}$$

By applying the matching conditions for the normal components of the dielectric displacements $\mathbf{D}$ at $z=0$ one finds

$$\sigma_S^+(\mathbf{Q},\omega)=-\sigma_S^-(\mathbf{Q},\omega)\equiv\sigma_S(\mathbf{Q},\omega), \tag{A4}$$

The continuity condition of the potential (A1) determines the value of the fictitious surface charge as

$$\begin{aligned}\sigma_S(\mathbf{Q},\omega)=&[\tilde{\varepsilon}_+^{-1}(\mathbf{Q},\omega)+\tilde{\varepsilon}_-^{-1}(\mathbf{Q},\omega)]^{-1}\int_{-\infty}^{\infty}dz'\rho_0(z',\mathbf{Q};\omega)\\&\times\{\theta(-z')[\tilde{\varepsilon}_-^{-1}(z',\mathbf{Q},\omega)+\tilde{\varepsilon}_-^{-1}(-z',\mathbf{Q},\omega)]\\&-\theta(z')[\tilde{\varepsilon}_+^{-1}(z',\mathbf{Q},\omega)+\tilde{\varepsilon}_+^{-1}(-z',\mathbf{Q},\omega)]\},\end{aligned} \tag{A5}$$

where we have introduced

$$\tilde{\varepsilon}_\pm^{-1}(z,\mathbf{Q},\omega)\equiv\frac{Q}{\pi}\int_{-\infty}^{\infty}dq_z\frac{e^{iq_zz}}{q^2\varepsilon_\pm(\mathbf{q},\omega)} \tag{A6}$$

and

$$\tilde{\varepsilon}_\pm^{-1}(\mathbf{Q},\omega)\equiv\tilde{\varepsilon}_\pm^{-1}(z=0,\mathbf{Q},\omega). \tag{A7}$$

Substituting Eqs. (A5) and (A3) into Eq. (A2) followed by a substitution of Eq. (A2) into Eq. (A1) yields the following expression for the total potential in the presence of the external charge

$$\phi(z,\mathbf{Q};\omega)=\int_{-\infty}^{\infty}dz'\,\alpha(z,z',\mathbf{Q};\omega)\rho_0(z',\mathbf{Q};\omega), \tag{A8}$$

where

$$\begin{aligned}\alpha(z,z',\mathbf{Q};\omega)=&\frac{2\pi}{Q}\{\theta(z)\,\theta(z')[\tilde{\varepsilon}_+^{-1}(z-z',\mathbf{Q},\omega)+\tilde{\varepsilon}_+^{-1}(z+z',\mathbf{Q},\omega)]+\theta(-z)\,\theta(-z')[\tilde{\varepsilon}_-^{-1}(z-z',\mathbf{Q},\omega)\\&+\tilde{\varepsilon}_-^{-1}(z+z',\mathbf{Q},\omega)]+[\theta(z)\tilde{\varepsilon}_+^{-1}(z,\mathbf{Q},\omega)-\theta(-z)\tilde{\varepsilon}_-^{-1}(z,\mathbf{Q},\omega)][\tilde{\varepsilon}_+^{-1}(\mathbf{Q},\omega)+\tilde{\varepsilon}_-^{-1}(\mathbf{Q},\omega)]^{-1}\\&\times(\theta(-z')[\tilde{\varepsilon}_-^{-1}(z',\mathbf{Q},\omega)+\tilde{\varepsilon}_-^{-1}(-z',\mathbf{Q},\omega)]-\theta(z')[\tilde{\varepsilon}_+^{-1}(z',\mathbf{Q},\omega)+\tilde{\varepsilon}_+^{-1}(-z',\mathbf{Q},\omega)])\}.\end{aligned} \tag{A9}$$

Since the external potential and the external charge distribution is related by

$$\rho_0(z,\mathbf{Q};\omega)=\frac{1}{4\pi}\left(Q^2-\frac{\partial^2}{\partial z^2}\right)\phi_{\text{ext}}(z,\mathbf{Q};\omega), \tag{A10}$$

we find that the inverse generalized dielectric function can be obtained as

$$\varepsilon^{-1}(z,z',\mathbf{Q};\omega)=\frac{1}{4\pi}\left(Q^2-\frac{\partial^2}{\partial z'^2}\right)\alpha(z,z',\mathbf{Q};\omega). \tag{A11}$$

Using the identity

$$\left(Q^2-\frac{\partial^2}{\partial z^2}\right)\tilde{\varepsilon}_{\pm}^{-1}(z,\mathbf{Q},\omega)=2Q\varepsilon_{\pm}^{-1}(z,\mathbf{Q},\omega), \tag{A12}$$

we then obtain

$$\begin{aligned}\varepsilon^{-1}(z,z',\mathbf{Q};\omega)=&\,\theta(z)\theta(z')[\varepsilon_+^{-1}(z-z',\mathbf{Q},\omega)+\varepsilon_+^{-1}(z+z',\mathbf{Q},\omega)]+\theta(-z)\theta(-z')[\varepsilon_-^{-1}(z-z',\mathbf{Q},\omega)+\varepsilon_-^{-1}(z+z',\mathbf{Q},\omega)]\\&+[\theta(z)\tilde{\varepsilon}_+^{-1}(z,\mathbf{Q},\omega)-\theta(-z)\tilde{\varepsilon}_-^{-1}(z,\mathbf{Q},\omega)][\tilde{\varepsilon}_+^{-1}(\mathbf{Q},\omega)+\tilde{\varepsilon}_-^{-1}(\mathbf{Q},\omega)]^{-1}\\&\times(\theta(-z')[\varepsilon_-^{-1}(z',\mathbf{Q},\omega)+\varepsilon_-^{-1}(-z',\mathbf{Q},\omega)]-\theta(z')[\varepsilon_+^{-1}(z',\mathbf{Q},\omega)+\varepsilon_+^{-1}(-z',\mathbf{Q},\omega)]).\end{aligned} \tag{A13}$$

By inserting the values $\varepsilon_+(\mathbf{q},\omega)=1$ and $\varepsilon_-(\mathbf{q},\omega)=\varepsilon(\mathbf{q},\omega)$ for the vacuum-solid interface, we finally arrive at the required expression, Eq. (3.22).

A different surface model was used in a recently published work by Chen and Chen.[22] In terms of our derivation, their model implies that Eq. (A3) should be replaced by

$$\rho_0^{\pm}(z,\mathbf{Q};\omega)=\rho_0(z,\mathbf{Q};\omega). \tag{A14}$$

A derivation of the generalized dielectric function for that model yields

$$\begin{aligned}\varepsilon^{-1}(z,z',\mathbf{Q};\omega)=&\,\theta(-z)\varepsilon_-^{-1}(z-z',\mathbf{Q},\omega)+\theta(z)\varepsilon_+^{-1}(z-z',\mathbf{Q},\omega)\\&+\frac{[\theta(z)\tilde{\varepsilon}_+^{-1}(z,\mathbf{Q},\omega)-\theta(-z)\tilde{\varepsilon}_-^{-1}(z,\mathbf{Q},\omega)][\varepsilon_-^{-1}(-z',\mathbf{Q},\omega)-\varepsilon_+^{-1}(-z',\mathbf{Q},\omega)]}{\tilde{\varepsilon}_+^{-1}(\mathbf{Q},\omega)+\tilde{\varepsilon}_-^{-1}(\mathbf{Q},\omega)},\end{aligned} \tag{A15}$$

which, after insertion of the conditions for the solid-vacuum interface, is transformed into Eq. (3.27).

*On leave from Zavoisky Physical-Technical Institute, Kazan, Russia.

[1] H. Raether, *in Excitation of Plasmon and Interband Transitions*, edited by G. Hofler, Springer Tracts in Modern Physics Vol. 88 (Springer-Verlag, New York, 1980).
[2] R. F. Egerton, *Electron Energy-Loss Spectroscopy in the Electron Microscope* (Plenum, New York, 1986).
[3] M. Inokuti, Rev. Mod. Phys. **43**, 297 (1971).
[4] D. P. Woodruff and T. A. Delchar, *Modern Techniques of Surface Science* (Cambridge University Press, New York, 1986)
[5] J. C. Riviere, *Surface Analytical Techniques* (Clarendon, Oxford, 1990)
[6] S. Tougaard and P. Sigmund, Phys. Rev. B **25**, 4452 (1982).
[7] A. L. Tofterup, Phys. Rev. B **32**, 2808 (1985).
[8] A. L. Tofterup, Surf. Sci. **227**, 157 (1990).
[9] V. M. Dwyer and J. A. D. Matthew, Surf. Sci. **193**, 549 (1988).
[10] I. S. Tilinin and W. S. M. Werner, Surf. Sci. **290**, 119 (1993).
[11] W. S. M. Werner, I. S. Tilinin, and M. Hayek, Phys. Rev. B **50**, 4819 (1994).
[12] J. Lindhard, K. Dan. Vidensk. Selsk. Mat. Fys. Medd. **28**(8) (1954).
[13] R. H. Ritchie, Phys. Rev. **106**, 874 (1957).
[14] L. Landau, J. Phys. (Moscow) **8**, 201 (1944).
[15] D. Mills, Surf. Sci. **48**, 59 (1975).
[16] T. Maniv and P. Gies, Surf. Sci. **211/212**, 242 (1989).
[17] K. Sturm, Adv. Phys. **31**, 1 (1982).
[18] V. Nazarov, Phys. Rev. B **49**, 10 663 (1994).
[19] F. Flores and F. Garcia-Moliner, J. Phys. C **12**, 907 (1979).
[20] F. Yubero and S. Tougaard, Phys. Rev. B **46**, 2486 (1992).
[21] F. Yubero, J. M. Sanz, B. Ramskov, and S. Tougaard, Phys. Rev. B **53**, 9719 (1996).
[22] Y. F. Chen and Y. T. Chen, Phys. Rev. B **53**, 4980 (1996).
[23] R. H. Ritchie and A. L. Marusak, Surf. Sci. **4**, 234 (1966).
[24] S. Dudarev, L.-M. Peng, and M. Whelan, Phys. Rev. B **48**, 13 408 (1993).
[25] L. Keldysh, Zh. Éksp. Teor. Fiz. **47**, 1515 (1964) [Sov. Phys. JETP **20**, 1018 (1965)].
[26] L. Kadanoff and G. Baym, *Quantum Statistical Mechanics* (Benjamin, New York, 1962); J. Rammer and H. Smith, Rev. Mod. Phys. **58**, 323 (1986); G. Mahan, *in Quantum Transport in Semiconductors*, edited by D. K. Ferry and C. Jacobony (Plenum Press, New York, 1991); A. P. Jauho, in *Quantum Transport in Semiconductors*, edited by D. K. Ferry and C. Jacobony (Plenum Press, New York, 1991).

[27] H. Kohl and H. Rose, in *Advances in Electronics and Electron Physics*, edited by P. W. Hawkes (Academic, Orlando, 1985).
[28] R. Ritchie, Phys. Rev. **114**, 644 (1959).
[29] E. Stern and R. Ferrell, Phys. Rev. **120**, 130 (1960).
[30] G. Mahan, Phys. Status Solidi B **55**, 703 (1973).
[31] P. A. Fedders, Phys. Rev. **153**, 438 (1967); P. J. Feibelman, *ibid.* **176**, 551 (1968); J. Harris and A. Griffin, Can. J. Phys. **48**, 2592 (1970); D. E. Beck, Phys. Rev. B **4**, 1555 (1971); J. F. Dobson and G. H. Harris, J. Phys. C **20**, 6127 (1987).
[32] N. J. M. Horing, E. Kamen, and H. L. Cui, Phys. Rev. B **32**, 2184 (1985).
[33] R. H. Ritchie and A. Howie, Philos. Mag. **36**, 463 (1977).
[34] P. C. Gibbons, S. E. Schnatterly, J. J. Ritsko, and J. R. Fields, Phys. Rev. B **13**, 2451 (1976).
[35] C. Kunz, Z. Phys. **196**, 311 (1966); A. Bagchi and C. B. Duke, Phys. Rev. B **5**, 2784 (1972).
[36] A. J. Bennett, Phys. Rev. B **1**, 203 (1970).
[37] A. A. Lucas, Phys. Rev. Lett. **26**, 229 (1971); A. A. Lucas and M. Sunjic, Prog. Surf. Sci. **2**, 75 (1972); E. Evans and D. L. Mills, Phys. Rev. B **5**, 4126 (1972); J. Schilling, Z. Phys. B: Condens. Matter **25**, 61 (1976).
[38] I. S. Tilinin, Zh. Éksp. Teor. Fiz. **82**, 1291 (1982) [Sov. Phys. JETP **55**, 751 (1982)].
[39] S. Tougaard and I. Chorkendorff, Phys. Rev. B **35**, 6570 (1987).
[40] F. Garcia-Moliner and F. Flores, *Introduction to the Theory of Solid Surfaces* (Cambridge University Press, Cambridge, England, 1979).
[41] J. L. Gervasoni and N. R. Arista, Surf. Sci. **260**, 329 (1992).